

CANCER

A reanalysis of nanoparticle tumor delivery using classical pharmacokinetic metrics

Lauren S. L. Price^{1,2*}, Stephan T. Stern³, Allison M. Deal⁴,
Alexander V. Kabanov^{1,5,6,7}, William C. Zamboni^{1,2,5,6,7†}

Nanoparticle (NP) delivery to solid tumors has recently been questioned. To better understand the magnitude of NP tumor delivery, we reanalyzed published murine NP tumor pharmacokinetic (PK) data used in the Wilhelm *et al.* study. Studies included in their analysis reporting matched tumor and blood concentration versus time data were evaluated using classical PK endpoints and compared to the unestablished percent injected dose (%ID) in tumor metric from the Wilhelm *et al.* study. The %ID in tumor was poorly correlated with standard PK metrics that describe NP tumor delivery ($AUC_{\text{tumor}}/AUC_{\text{blood}}$ ratio) and only moderately associated with maximal tumor concentration. The relative tumor delivery of NPs was ~100-fold greater as assessed by the standard $AUC_{\text{tumor}}/AUC_{\text{blood}}$ ratio than by %ID in tumor. These results strongly suggest that PK metrics and calculations can influence the interpretation of NP tumor delivery and stress the need to properly validate novel PK metrics against traditional approaches.

INTRODUCTION

The theoretical advantages of nanoparticles (NPs) in cancer treatment include increased solubility, prolonged duration of exposure, selective delivery to the tumor, and an improved therapeutic index of the encapsulated or conjugated drug (1, 2). The number of available NP-based drug delivery systems for the treatment of cancer and other diseases has seen exponential growth in the past three decades. In 2017 alone, there were more than 300 nanomedicine patent filings, with more than half related to drug delivery (3). While the number of NP-based agents used clinically is still limited, the plethora that is emerging as potential therapeutic agents warrants the need for detailed studies of their unique pharmacology in animal models and in humans. Doxil, Onivyde, and Abraxane are the only members of this relatively new class of drugs that are approved by the Food and Drug Administration (FDA) for the treatment of solid tumors and currently available on the U.S. market. Despite the regulatory success of these drugs, the promise of NP-based agents for the treatment of cancer remains unfulfilled because of several factors including potential overall low tumor delivery (4, 5).

The disposition of NPs is dependent on the carrier and not on the therapeutic entity until the drug is released (6, 7). This complexity required the creation of nomenclature to describe NP pharmacokinetics (PK), including encapsulated or conjugated (the drug within or bound to the carrier), released (active drug that no longer associates with the carrier), and sum total or total (encapsulated/conjugated drug plus released drug) (6, 8). NPs act as prodrugs and are not active

until the small-molecule (SM) drug is released from the carrier. In theory, the PK disposition of the drug after release from the carrier is the same as after administration of the SM formulation (6). Examples of various types of NPs include liposomes, polymeric micelles, fullerenes, carbon nanotubes, quantum dots, nanoshells, polymers, dendrimers, and conjugates, including antibody-drug conjugates (9). Thus, the types of NP carriers are vast and highly variable, and each type may have unique biological interactions and PK characteristics (10). As a result, detailed analytical studies must be performed to assess the disposition of encapsulated/conjugated and released forms of the drug in plasma, tumor, and tissues as part of PK and biodistribution studies in animals and patients (7). However, there are currently few, if any, robust and validated bioanalytical methods capable of quantifying released drug in tumors and tissues, which limits the ability to fully characterize the disposition of NP-based agents and compare them to conventional SM formulations (11). This has led to a limited number of published studies that evaluated the PK of NP encapsulated/conjugated and released drug in tumors. However, the use of modeling and simulation approaches to characterize this complex interplay is also emerging (12).

In theory, size-selective permeability of the tumor vasculature allows NPs to enter the tumor interstitial space, while suppressed lymphatic filtration prevents clearance, resulting in accumulation. This phenomenon, termed the enhanced permeability and retention (EPR) effect, may be exploited by NPs to deliver drugs to tumors (4, 5, 13). Unfortunately, progress in developing effective NPs relying on this approach has been hampered by heterogeneity of the EPR effect and lack of information on factors that influence EPR (4, 5, 14). Cancer cells in tumors are surrounded by a complex microenvironment composed of endothelial cells of the blood and lymphatic circulation, stromal fibroblasts, collagen, cells of the mononuclear phagocyte system, and other immune cells. Each of these components is a potential barrier to tumor delivery and intratumoral distribution of NPs and may be associated with variability in EPR (4, 14–17). In addition, these potential barriers may be highly variable both within and across tumors, which further increases heterogeneity in the EPR effect. Thus, all solid tumors may not be conducive for treatment by NPs, which rely on EPR for delivery.

¹Carolina Center of Cancer Nanotechnology Excellence (C-CCNE), University of North Carolina, Chapel Hill, NC, USA. ²Translational Oncology and Nanoparticle Drug Development (TOND2I) Lab, University of North Carolina, Chapel Hill, NC, USA. ³Nanotechnology Characterization Lab (NCL), Frederick National Laboratory for Cancer Research, Frederick, MD, USA. ⁴UNC Lineberger Biostatistics Shared Resource, Chapel Hill, NC, USA. ⁵UNC Lineberger Comprehensive Cancer Center, Chapel Hill, NC, USA. ⁶Center for Nanotechnology in Drug Delivery, UNC Eshelman School of Pharmacy, Chapel Hill, NC, USA. ⁷Carolina Institute for Nanomedicine, University of North Carolina, Chapel Hill, NC, USA.

*Present address: Division of Cancer Pharmacology II, Office of Clinical Pharmacology, Office of Translational Sciences, Center for Drug Evaluation and Research, US Food and Drug Administration, Silver Spring, MD, USA.

†Corresponding author. Email: zamboni@email.unc.edu

A workshop by the Alliance for Nanotechnology in Cancer concluded that there are major gaps in the understanding of factors that affect and inhibit EPR effect and NP tumor delivery, and new fundamental preclinical and clinical studies in this area are needed to effectively advance NP drug delivery and efficacy in solid tumors (4). Recent meta-analyses, described in detail below, have reported lower than expected NP tumor delivery, highlighting the potential limitations of current EPR-based NP delivery to tumors and the need to systematically evaluate NP disposition (18, 19).

Despite great promise, the impact of NPs on the treatment of solid tumors in patients, and in some cases, preclinical models, has been limited. To evaluate NP tumor delivery as compared to SM drugs, our group previously conducted a meta-analysis evaluating the plasma and tumor PK of NPs and SM anticancer agents using both standard PK parameters and a PK metric called “relative distribution index over time (RDI-OT)” that measures efficiency of tumor delivery (18). In general, standard PK parameters such as plasma and tumor C_{\max} and area under the time concentration curves (AUCs) were higher for NP agents than their respective SM drugs, as expected. However, when examining measures of tumor delivery efficiency, NPs underperform compared to SM drugs. $AUC_{\text{tumor}}/AUC_{\text{plasma}}$ ratio was higher for the SM drug compared to the NP formulation for 14 of 17 datasets, and similar to this traditional PK approach, every SM tumor RDI-OT AUC_{0-6h} value was also greater than that of its comparator NP. The lower efficiency of delivery seen with NPs compared with SMs suggests that even though NPs can deliver an overall greater total drug exposure to the tumor, there may be a limit to the extent or amount of NPs that can enter tumors (18). An important caveat to this conclusion, however, is that active, released NP drug concentrations were not evaluated, and without this key component of the PK analysis, it is impossible to infer potential advantages or disadvantages of the NP-mediated tumor delivery in comparison to SM. Regardless, the extent of NP-mediated tumor delivery estimated in our study, with a median $AUC_{\text{tumor}}/AUC_{\text{plasma}}$ ratio of 0.4 (i.e., tumor exposure was 40% of plasma exposure), was still much higher than suggested in a recent study by Wilhelm *et al.* that attempted to relate NP tumor exposure to the injected dose, with a median estimated tumor value of 0.7% of the injected dose.

Wilhelm *et al.* (19) recently performed a meta-analysis evaluating the percentage of injected dose (%ID) of NPs that reaches the tumor from 117 published preclinical studies. The results of this analysis were somewhat unexpected and disappointing in that a median of only 0.7 %ID of NPs was found to be delivered to a solid tumor. The authors concluded that this overall low tumor delivery has negative consequences for the translation of nanotechnology for human use with respect to manufacturing, cost, toxicity, and imaging and therapeutic efficacy. However, there were several limitations to this study, such as highly variable study designs in the source publications, which included differences in dosing regimens, sampling schemes (especially limited sample numbers or short sampling durations), sample processing and analytical methods (limited data on exposures of active-released drug in tumors), and, in some cases, absence of matched blood PK data. The study was criticized in a follow-up perspective article by McNeil (20) that argued that the PK analysis used by Wilhelm *et al.* may be flawed because of the use of non-traditional methods. The tumor delivery efficiency in the Wilhelm *et al.* study was estimated using an unestablished PK metric, %ID in tumor, that was not supported by traditional PK analysis. The %ID in tumor

parameter, calculated as $\%ID \text{ in tumor} = (AUC_{\text{tumor}}/t_{\text{end}}) * \text{tumor mass}$, is not a true measure of tissue exposure or delivery efficiency, because it reduces the time-concentration series to a single average drug mass value that neglects exposure time and does not relate tumor and systemic exposures. Further, the %ID in tumor metric is heavily influenced by the time points and total duration used in the estimation, and this single mass value does not reflect the overall PK disposition of a NP. Traditional comparison of AUC_{tumor} to AUC_{blood} ($AUC_{\text{tumor}}/AUC_{\text{blood}}$ ratio) is considerably more meaningful because it takes into account the entire time-concentration series and relates tumor exposure to systemic exposure.

The goal of our current study was to compare the tumor disposition of NPs as depicted by the nonstandard %ID in tumor PK metric generated by Wilhelm *et al.* compared with standard PK metrics. In the present reanalysis, we compiled the source data from the 117 NP PK studies in mice that were evaluated in the original Wilhelm *et al.* study and then extracted and analyzed those studies that included matched tumor and blood concentration versus time data. We then compared established PK parameters resulting from the reanalysis of these extracted data to the %ID in tumor metric used in the prior study by Wilhelm *et al.* The %ID in tumor metric was found to correlate very poorly with established PK measures of exposure and delivery efficiency in tumors. These data refute the use of the exposure term %ID in tumor in the Wilhelm *et al.* study and suggest that the resulting conclusions regarding the efficiency of NP tumor distribution were misleading. The results of our present reanalysis support the use of established PK approaches and metrics to evaluate NP tumor delivery and stress the necessity to properly validate novel metrics against traditional PK metrics using standard methods.

RESULTS

Summary of datasets evaluated

From the 117 articles included in the data analysis by Wilhelm *et al.*, 256 NP PK datasets were identified and evaluated. A total of 136 unique datasets contained sufficient data for calculation of both blood and tumor PK parameters and were included in the analysis. Each dataset included PK data collected following a single intravenous dose of a NP agent to tumor-bearing mice. The majority of included studies were conducted in xenograft models (120 of 136 datasets) with a smaller proportion in orthotopic models (13 of 136 datasets).

Relationship between %ID in tumor and established PK parameters for all NPs

The relationship between the Wilhelm *et al.* %ID in tumor PK metric and established PK parameters, $AUC_{\text{tumor}}/AUC_{\text{blood}}$ ratio, RDI-OT AUC_{tumor} , and tumor C_{\max} for all NP types combined, is presented in Fig. 1. The Spearman correlation coefficients and Pearson correlation coefficients for these relationships are included in tables S1 and S2, respectively. Including different types of NPs together, there was no relationship between %ID in tumor and $AUC_{\text{tumor}}/AUC_{\text{blood}}$ ratio, a weak relationship between %ID in tumor and RDI-OT AUC_{tumor} , and a moderate relationship between %ID in tumor and tumor C_{\max} , based on p value (see Materials and Methods for criteria). For all NP types combined, the median and interquartile range of values for %ID in tumor, $AUC_{\text{tumor}}/AUC_{\text{blood}}$ ratio (as a percentage), RDI-OT AUC_{tumor} , and tumor C_{\max} are presented in Table 1. The median (interquartile range) for %ID in tumor was 0.67% (0.36 to 1.19%) and that for $AUC_{\text{tumor}}/AUC_{\text{blood}}$ ratio was 76.12% (48.79 to 158.81%).

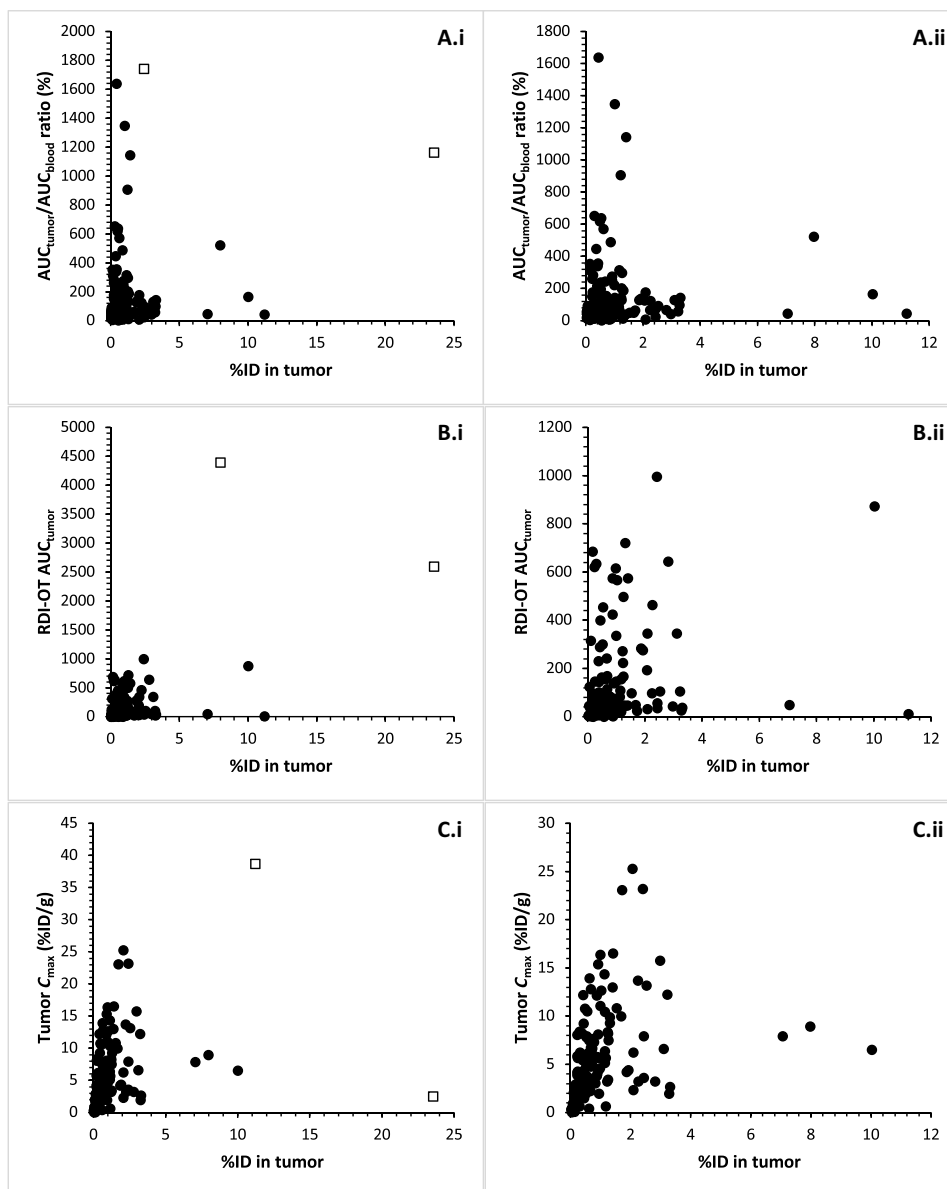


Fig. 1. Comparisons between %ID in tumor and traditional PK metrics for all datasets (i.e., all types of nanoparticles). Correlation plots for all datasets between %ID in tumor (per Wilhelm *et al.*) and $AUC_{\text{tumor}}/AUC_{\text{blood}}$ ratio (%) (A), RDI-OT AUC_{tumor} (B), and tumor C_{max} (C). Plots are shown with all datasets (i, outliers shown as \square) and with outliers excluded (ii). There was no relationship between %ID in tumor and $AUC_{\text{tumor}}/AUC_{\text{blood}}$ ratio (%) [$\rho = 0.183$ all data (AD); $\rho = 0.151$ excluding outliers (EO)] and a weak relationship between %ID in tumor and RDI-OT AUC_{tumor} ($\rho = 0.319$ AD; $\rho = 0.289$ EO). There was a moderate relationship between %ID in tumor and the tumor C_{max} ($\rho = 0.562$ AD; $\rho = 0.572$ EO).

Relationship between %ID in tumor and established PK parameters for liposomes

The relationship between the Wilhelm *et al.* %ID in tumor estimation and established PK parameters, $AUC_{\text{tumor}}/AUC_{\text{blood}}$ ratio, RDI-OT AUC_{tumor} , and tumor C_{max} , for the liposomal NP subset is presented in Fig. 2. The Spearman correlation coefficients and Pearson correlation coefficients for these relationships are included in tables S1 and S2, respectively. For the liposomal NP subset, there was no relationship between %ID in tumor and $AUC_{\text{tumor}}/AUC_{\text{blood}}$ ratio, no relationship between %ID in tumor and RDI-OT AUC_{tumor} , and a weak relationship between %ID in tumor and tumor C_{max} , based

on ρ value (see Materials and Methods for criteria). For liposomes, the median and interquartile range of values for %ID in tumor, $AUC_{\text{tumor}}/AUC_{\text{blood}}$ ratio as a percentage, RDI-OT AUC_{tumor} , and tumor C_{max} are presented in Table 1. The median (interquartile range) for %ID in tumor was 0.55% (0.31 to 2.17%) and that for $AUC_{\text{tumor}}/AUC_{\text{blood}}$ ratio was 45.46% (31.16 to 63.48%).

Relationship between %ID in tumor and established PK parameters for polymeric NPs

The relationship between the Wilhelm *et al.* %ID in tumor estimation and established PK parameters, $AUC_{\text{tumor}}/AUC_{\text{blood}}$ ratio, RDI-OT

Table 1. Median and interquartile range values for all calculated PK metrics.

Median (interquartile range)	All subsets combined	Liposome subset	Polymeric subset	Inorganic subset
%ID in tumor	0.67 (0.36–1.19)	0.55 (0.31–2.17)	0.68 (0.42–1.26)	0.64 (0.35–1.14)
AUC _{tumor} /AUC _{blood} ratio (%)	76.12 (48.79–158.81)	45.46 (31.16–63.48)	143.94 (56.00–318.87)	81.44 (55.01–135.92)
RDI-OT AUC _{tumor}	59.64 (26.54–158.60)	74.63 (39.77–100.89)	48.69 (23.55–160.48)	63.75 (26.68–209.85)
Tumor C _{max} (%ID/g)	4.71 (2.65–7.97)	3.92 (2.71–7.07)	6.26 (3.05–10.22)	4.21 (2.46–6.57)

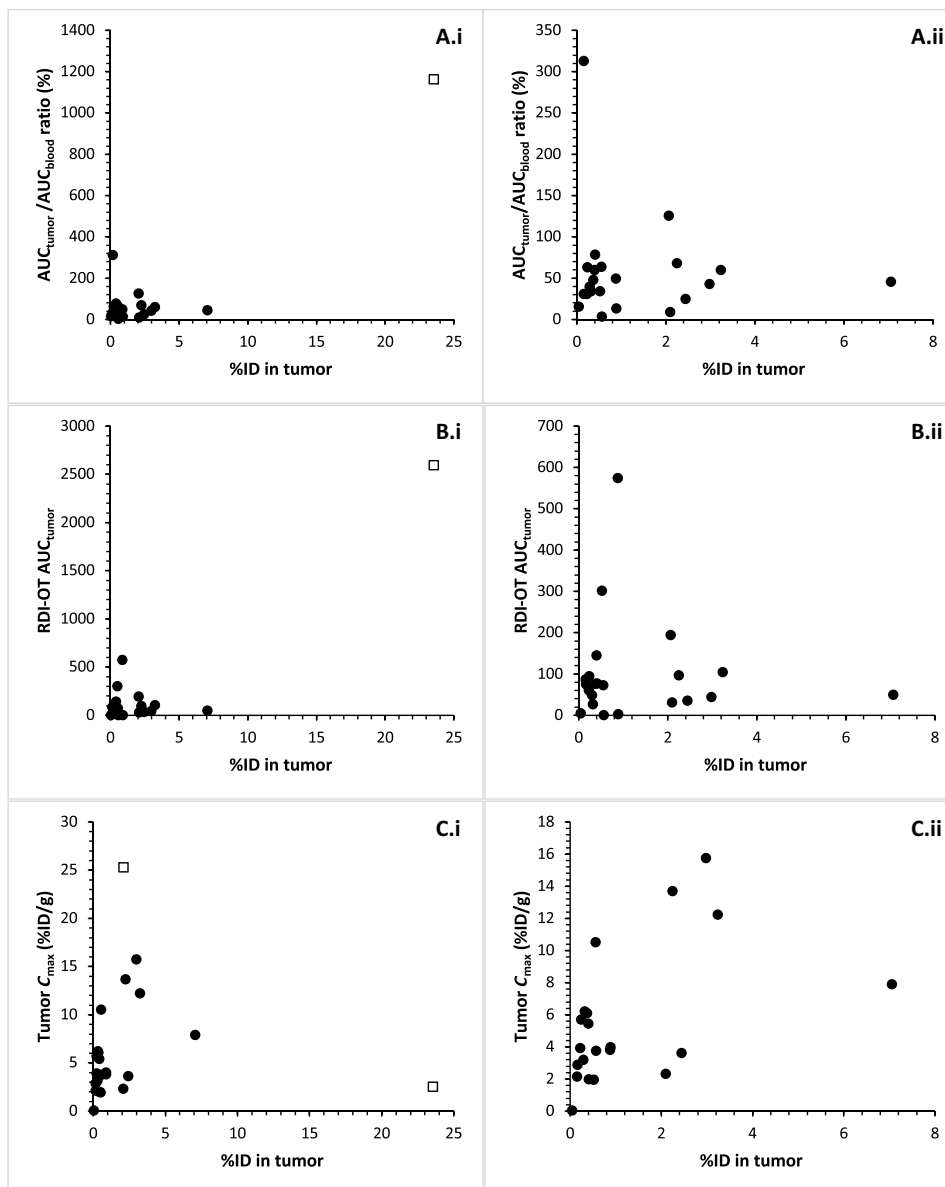


Fig. 2. Comparisons between %ID in tumor and traditional PK metrics in the liposome subset. Correlation plots for the liposome subset between %ID in tumor (per Wilhelm *et al.*) and AUC_{tumor}/AUC_{blood} ratio (%) (A), RDI-OT AUC_{tumor} (B), and tumor C_{max} (C). Plots are shown with all liposome datasets (i, outliers shown as □) and with outliers excluded (ii). There was no relationship between %ID in tumor and AUC_{tumor}/AUC_{blood} ratio (%) ($\rho = 0.145$ AD; $\rho = 0.023$ EO) and no relationship between %ID in tumor and RDI-OT AUC_{tumor} ($\rho = 0.150$ AD; $\rho = 0.029$ EO). There was a weak relationship between %ID in tumor and the tumor C_{max} ($\rho = 0.412$ AD; $\rho = 0.514$ EO).

AUC_{tumor} , and tumor C_{max} , for the polymeric NP subset is presented in Fig. 3. The Spearman correlation coefficients and Pearson correlation coefficients for these relationships are included in tables S1 and S2, respectively. For the polymeric NP subset, there was no relationship between %ID in tumor and $AUC_{\text{tumor}}/AUC_{\text{blood}}$ ratio, a weak relationship between %ID in tumor and RDI-OT AUC_{tumor} , and a moderate relationship between %ID in tumor and tumor C_{max} , based on ρ value (see Materials and Methods for criteria). For polymeric NPs, the median and interquartile range of values for %ID in tumor, $AUC_{\text{tumor}}/AUC_{\text{blood}}$ ratio as a percentage, RDI-OT AUC_{tumor} , and tumor C_{max} are presented in Table 1. The median (interquartile range) for %ID in tumor was 0.68% (0.42 to 1.26%) and that for $AUC_{\text{tumor}}/AUC_{\text{blood}}$ ratio was 143.94% (56.00 to 318.87%).

Relationship between %ID in tumor and established PK parameters for inorganic NPs

The relationship between the Wilhelm *et al.* %ID in tumor estimation and established PK parameters, $AUC_{\text{tumor}}/AUC_{\text{blood}}$ ratio, RDI-OT AUC_{tumor} , and tumor C_{max} , for the inorganic NP subset is presented in Fig. 4. Spearman correlation coefficients and Pearson correlation coefficients for these relationships are included in tables S1 and S2, respectively. For inorganic NPs, there was no relationship between %ID in tumor and $AUC_{\text{tumor}}/AUC_{\text{blood}}$ ratio, a weak relationship between %ID in tumor and RDI-OT AUC_{tumor} , and a moderate relationship between %ID in tumor and tumor C_{max} , based on ρ value (see Materials and Methods for criteria). For inorganic NPs, the median and interquartile range of values for %ID in tumor, $AUC_{\text{tumor}}/AUC_{\text{blood}}$

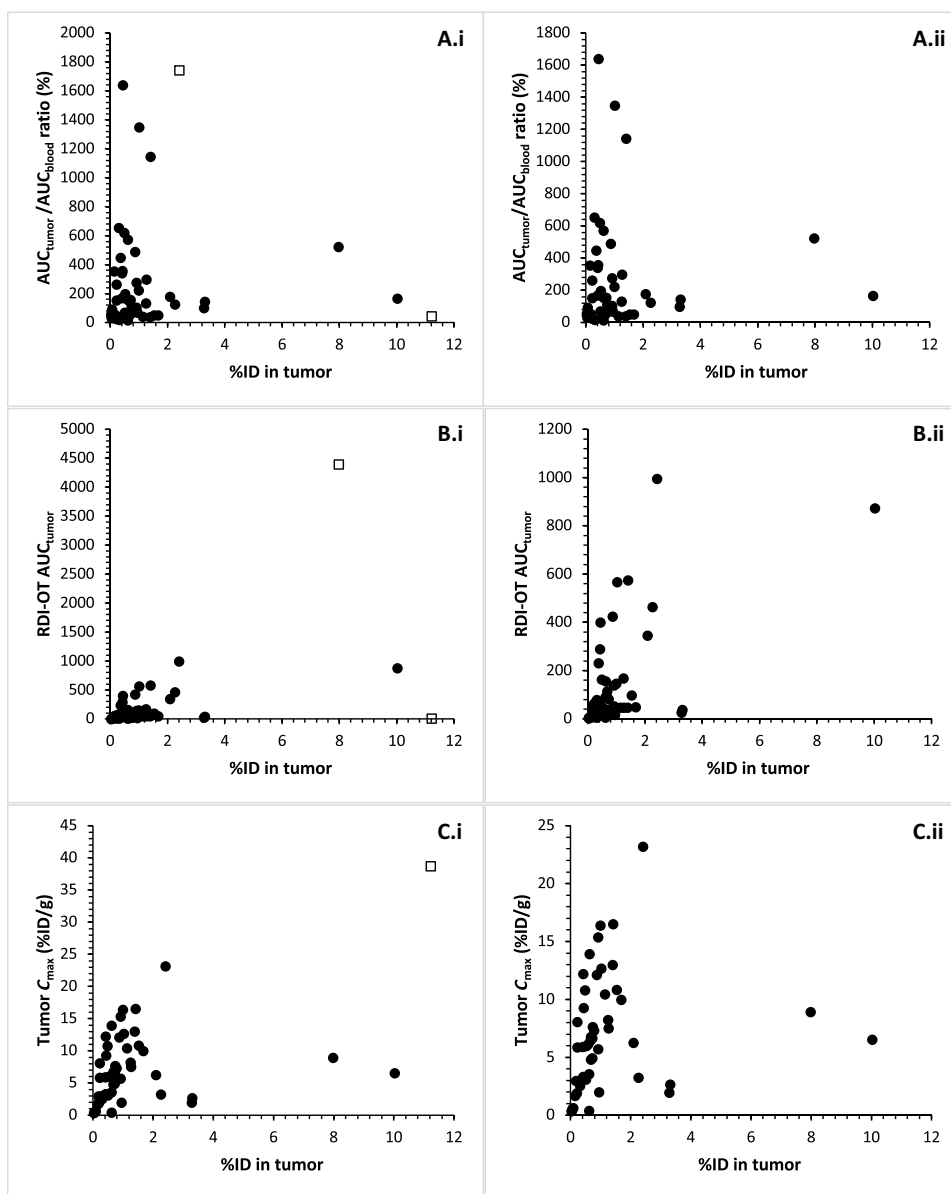


Fig. 3. Comparisons between %ID in tumor and traditional PK metrics in the polymeric subset. Correlation plots for the polymeric subset between %ID in tumor (per Wilhelm *et al.*) and $AUC_{\text{tumor}}/AUC_{\text{blood}}$ ratio (%) (A), RDI-OT AUC_{tumor} (B), and tumor C_{max} (C). Plots are shown with all polymeric datasets (i, outliers shown as \square) and with outliers excluded (ii). There was no relationship between %ID in tumor and $AUC_{\text{tumor}}/AUC_{\text{blood}}$ ratio (%) ($\rho = 0.094$ AD; $\rho = 0.097$ EO) and a weak relationship between %ID in tumor and RDI-OT AUC_{tumor} ($\rho = 0.422$ AD; $\rho = 0.447$ EO). There was a moderate relationship between %ID in tumor and the tumor C_{max} ($\rho = 0.547$ AD; $\rho = 0.519$ EO).

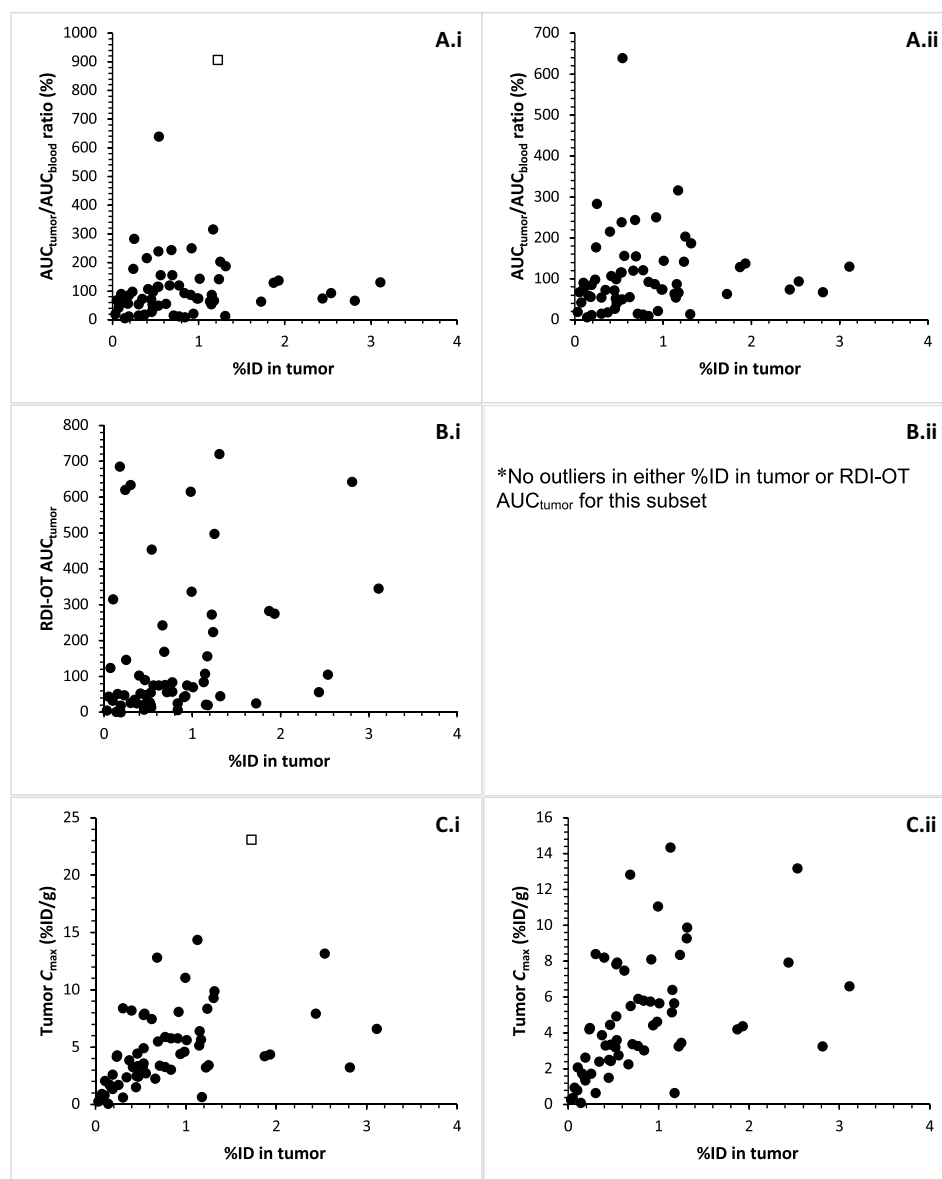


Fig. 4. Comparisons between %ID in tumor and traditional PK metrics in the inorganic subset. Correlation plots for the inorganic subset between %ID in tumor (per Wilhelm *et al.*) and $AUC_{\text{tumor}}/AUC_{\text{blood}}$ ratio (%) (A), RDI-OT AUC_{tumor} (B), and tumor C_{max} (C). Plots are shown with all inorganic datasets (i, outliers shown as \square) and with outliers excluded (ii). There was no relationship between %ID in tumor and $AUC_{\text{tumor}}/AUC_{\text{blood}}$ ratio (%) ($\rho=0.265$ AD; $\rho=0.243$ EO) and a weak relationship between %ID in tumor and RDI-OT AUC_{tumor} ($\rho=0.322$ AD). There was a moderate relationship between %ID in tumor and the tumor C_{max} ($\rho=0.618$ AD; $\rho=0.605$ EO).

ratio as a percentage, RDI-OT AUC_{tumor} , and tumor C_{max} are presented in Table 1. The median (interquartile range) for %ID in tumor was 0.64% (0.35 to 1.14%) and that for $AUC_{\text{tumor}}/AUC_{\text{blood}}$ ratio was 81.44% (55.01 to 135.92%).

DISCUSSION

Currently, only three NP-based anticancer agents are FDA-approved for treatment of solid tumors. Both the pharmacology of NPs and the physiology of solid tumors are complex, and the interactions between the two are not fully understood. Recent analyses have questioned the utility of NPs for the treatment of solid tumors due to potential low tumor delivery efficiency and extent, especially the often-cited study by Wilhelm *et al.* (19) However, the conclusions

of the study by Wilhelm *et al.* were based on a nonstandard PK metric, %ID in tumor, which was several orders of magnitude lower than other published PK metrics describing the tumor delivery efficiency of SM and NP drugs (18). To better characterize the delivery of drug-loaded NPs to solid tumors, we compiled and analyzed the source data from the published NP PK studies in mice used by the Wilhelm *et al.* study and evaluated the relationship between established PK parameters describing the tumor disposition of NP agents and the novel %ID in tumor metric. The goal of this study was to directly compare the relationship and absolute values of these PK metrics and consider how these values influence the interpretation of results.

Our findings reinforce the importance of adequate study design and PK metric selection when investigating NP PK. The calculation of %ID in tumor by Wilhelm *et al.* differs from the standard calculation

of %ID. The conventional calculation of tissue %ID represents the amount of drug in the target tissue at a single time point and is calculated as follows

$$\%ID = 100 * (\text{Amount of drug or decay corrected activity in tissue}) / \text{Dose}$$

The calculation of %ID in tumor used by Wilhelm *et al.* begins with AUC_{tumor} (in units of hours*%ID/g) and cancels units (dividing by t_{last} in hours and multiplying by tumor mass in grams) to arrive at final units of %ID. Given that the duration of PK studies are generally greater than 1 hour and the size of tumors in mouse models are typically less than 1 g, modifying or normalizing the AUC_{tumor} by these values (e.g., divide by 72 hours, which is the duration of the PK study; multiply by 0.2 g, which is the size of the tumor) results in progressively smaller values. Rather than representing the total amount of drug in the tumor at a single time point (as used by conventional calculations of %ID), this nonstandard calculation actually describes the average amount of drug in the tumor within separate 1-hour intervals throughout the entire PK evaluation period.

By time-averaging and converting to drug mass, the Wilhelm *et al.* calculation excludes the important pharmacological concepts of drug concentration (i.e., law of mass action), exposure duration, and relative distribution (i.e., on/off target exposure) that are fundamental to understanding drug effect. Thus, the %ID in tumor metric is difficult to interpret, as it is not a measure of how much available drug distributes to the tumor, or even how much injected drug distributes to the tumor (as it has been interpreted). The inference from the %ID in tumor calculation is that perfect tumor uptake would be 100 %ID in tumor, but that would only be the case if the entire injected dose of drug instantaneously distributed to the tumor and remained in the tumor over the entire observation period without clearing, based on the calculations used. To clarify this point, using this calculation, systemic exposure itself upon intravenous injection would only be 100 %ID if the drug circulated indefinitely and never cleared. Obviously, this is a very flawed calculation. Established PK metrics that describe the extent and efficiency of NP tumor delivery take into account both the systemic (blood or plasma) and tumor exposure (i.e., drug concentration and duration, AUC). An example of standard PK metric and %ID in tumor calculations from blood and tumor concentration versus time profiles is shown in Fig. 5. The mock dataset portrayed by the solid lines represents approximately median values for %ID in tumor (0.7 %ID) and $AUC_{\text{tumor}}/AUC_{\text{blood}}$ ratio (70%) assuming a tumor mass of 0.2 g. The dotted lines represent the approximate interquartile ranges. Given that the %ID in tumor metric ignores systemic exposure, any degree of change in AUC_{blood} does not affect the calculation or interpretation of the %ID in tumor metric. In contrast, $AUC_{\text{tumor}}/AUC_{\text{blood}}$ ratio is, by definition, sensitive to changes in either or both systemic exposure and target tissue exposure. These differences highlight the disconnect between the %ID in tumor metric and standard PK parameters and explain the lack of relationship between parameters identified in this analysis. This example and our results show how the use of non-standard PK metrics can markedly alter the interpretation of drug delivery to tumors.

Not only was the %ID in tumor metric used by Wilhelm *et al.* a nonstandard calculation of %ID, it was also found not to be related to other standard PK parameters. The %ID in tumor metric used by Wilhelm *et al.* was not related to the more commonly and historically used PK metric describing the extent of tumor delivery (i.e., $AUC_{\text{tumor}}/AUC_{\text{blood}}$ ratio). This observation was consistent for the full dataset and all three subsets (liposomes, polymeric NPs, or inorganic NPs),

whether outliers were included or excluded. However, the %ID in tumor calculated by Wilhelm *et al.* could have been measuring a different process, such as efficiency of delivery. Similarly, there was a weak or no relationship between %ID in tumor and a metric of efficiency of tumor delivery (i.e., RDI-OT AUC_{tumor}). Furthermore, the absolute values and resultant interpretations of these metrics differ substantially. The median %ID in tumor for all subsets combined was 0.67 %ID, while the median $AUC_{\text{tumor}}/AUC_{\text{blood}}$ ratio was 76.12%. Per Wilhelm *et al.*, this %ID in tumor was interpreted as only 7 of every 1000 administered NPs entering the tumor, a disappointingly low NP delivery. As described above, a more accurate description would be that an average of 0.67% of the injected dose could be found in the tumor at every 1-hour interval throughout the entire PK evaluation period. Using the more appropriate $AUC_{\text{tumor}}/AUC_{\text{blood}}$ ratio metric from the same datasets, the PK results have a completely different and ultimately far more positive interpretation. For example, with an $AUC_{\text{tumor}}/AUC_{\text{blood}}$ ratio of 76.12%, the overall exposure of NP in the tumor (AUC_{tumor}) was 76.12% of the overall exposure in the plasma (AUC_{blood}), which is a much more promising result.

There was a moderate relationship between %ID in tumor and tumor C_{max} . Again, %ID in tumor resulted in substantially smaller absolute values (median, 0.67 %ID; interquartile range, 0.36 to 1.19 %ID) than tumor C_{max} (median, 4.71 %ID/g; interquartile range, 2.65 to 7.97 %ID/g). Given that the tumor C_{max} directly contributes to the calculation of AUC_{tumor} and, in turn, %ID in tumor, the moderate relationship is expected. As opposed to the two previously described metrics ($AUC_{\text{tumor}}/AUC_{\text{blood}}$ ratio and RDI-OT AUC_{tumor}), both %ID in tumor and tumor C_{max} exclusively evaluate the disposition of the NP in tumor without considering the systemic disposition and are therefore of lower utility to describe the extent or efficiency of NP tumor delivery.

Our study has several limitations and factors to consider. The source studies included in this analysis were limited to those previously identified and evaluated by Wilhelm *et al.* to provide a direct comparison of PK metric results and interpretations. There are many additional published NP PK studies that did not meet the selection criteria or were not identified in the initial evaluation. In addition, the calculations completed in this analysis rely on the quality and accuracy of the data collected and published by the authors in the source studies. The study designs, analytical methods, and measured moieties may all influence the results and interpretation of PK data. For example, simply excluding those studies with no matching blood concentration data reported decreased the overall sample size of our analysis by approximately one-third relative to the original analysis by Wilhelm *et al.* Another important issue is that most of these studies measured total drug (i.e., encapsulated plus released), and not the biologically active, released drug fraction. Although encapsulated drug dominates the total drug profile for most NP formulations, and therefore, NP-encapsulated tumor uptake can be inferred from the total drug profile, it is the released drug fraction that correlates with toxicity and efficacy (7).

Despite these limitations, our study provides direct comparison of PK metrics calculated from identical source data and highlights how the interpretation of NP PK results can be markedly influenced by the differing PK metrics selected. For example, the median (interquartile range) for %ID in tumor was 0.67 %ID (0.36 to 1.19%) and that for $AUC_{\text{tumor}}/AUC_{\text{blood}}$ ratio was 76.12% (48.79 to 158.81%). The median values for %ID in tumor and $AUC_{\text{tumor}}/AUC_{\text{blood}}$ ratio were 113-fold different, and thus, metric selection greatly influences

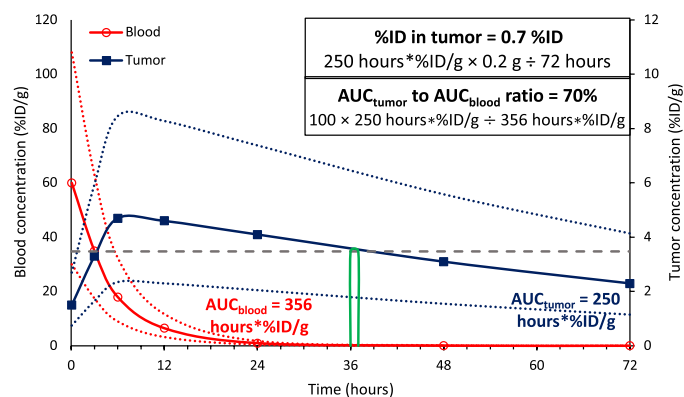


Fig. 5. Example concentration versus time profiles of NPs in blood (left y axis) and tumor (right y axis) and PK metric calculation. The concentration versus time profile in blood is represented by the red symbols and lines. The concentration versus time profile in tumor is represented by the blue symbols and lines. The dotted red and blue lines represent the approximate variability in interquartile range for the blood and tumor concentration versus time profiles, respectively. The dashed gray line represents a constant tumor concentration of 3.5 %ID/g that yields the same AUC_{tumor} (250 hours*%ID/g) as the actual tumor concentration versus time profile. The %ID in tumor calculated by Wilhelm *et al.* of 0.7% is the average %ID found in the tumor at every 1-hour interval throughout the entire PK evaluation period and is represented by the vertical white and green bar.

the interpretation of the results and the conclusion of the study. Optimal study design, including analysis of both tumor and blood concentrations, is critical to understanding the efficiencies and deficiencies of NP tumor delivery.

To fully evaluate the current and potential impact of NPs on the treatment of solid tumors, more detailed and extensive meta-analyses, modeling, and statistical comparisons, ideally using PK datasets that include all drug fractions (i.e., total, encapsulated, and released drug), are needed to evaluate and predict what NP formulation attributes, dosing regimens, and animal model characteristics are associated with high tumor delivery and efficacy of NPs for solid tumor treatment.

MATERIALS AND METHODS

Data extraction

All 117 articles included in the data analysis by Wilhelm *et al.* (19) were accessed and reviewed. Each identifiable dataset was given a unique identifier, and data were extracted from published text, tables, and figures for inclusion in a comprehensive database. Retrieved information included NP specifications (NP type and encapsulated or conjugated drug) and PK study data (dose, route, regimen, analytical methods, and concentration versus time data for tumor and blood or plasma). When available, concentration data were preferentially sourced from published text or tables (including the Supplementary Materials). If numerical concentration data were not published in text or tables, WebPlotDigitizer version 3.12 (Ankit Rohatgi, Austin, TX) was used to extract data from concentration versus time plots.

PK metric calculation

Following data extraction, the raw concentration versus time data were used to calculate various PK metrics for each unique dataset. When needed, data were converted to units of %ID/g using assump-

tions published by Wilhelm *et al.* The tumor AUC and delivery efficiency (%ID) were calculated per Wilhelm *et al.* (19). For clarity, the Wilhelm *et al.* delivery efficiency metric is described as “%ID in tumor” throughout this analysis. In addition, the blood AUC was calculated by the linear trapezoidal rule (to match tumor AUC calculations) from 0 to t_{last} . The ratio of tumor AUC to blood AUC was calculated as follows

$$AUC_{tumor}/AUC_{blood} \text{ ratio} (\%) = 100 * AUC_{tumor} (\text{hours} * \%ID/g_{tumor}) / AUC_{blood} (\text{hours} * \%ID/g_{blood})$$

The RDI-OT, used to evaluate the efficiency of tumor delivery from systemic circulation, is calculated as the ratio of tumor concentration to blood concentration at the same time point (e.g., 24 hours) (18). The area under the tumor RDI-OT curve (RDI-OT AUC_{tumor}) from 0 to t_{last} was calculated using the linear trapezoidal rule for each dataset. Last, the tumor C_{max} was determined by visual inspection.

Study exclusion and statistical analysis

After data extraction and PK metric calculation, each unique dataset was assessed for inclusion in the final analysis. Datasets were excluded if there were missing, incomplete, insufficient (i.e., <3 time points), or unmatched tumor and blood data, or if units could not be converted to %ID/g. In addition, datasets representing NPs administered by nonintravenous routes (i.e., intraperitoneal or subcutaneous), to animals other than mice, or those with duplicate data were excluded.

All remaining datasets were evaluated in the final analysis. For each metric, outliers were identified by the Grubbs’ test ($P < 0.01$). The correlation between PK metrics used by Wilhelm *et al.* (%ID in tumor) and standard PK metrics (AUC_{tumor}/AUC_{blood} ratio and tumor C_{max}) and tumor delivery efficiency metrics (RDI-OT AUC_{tumor}) was estimated using Spearman’s rank correlation coefficients (ρ) and Pearson correlation coefficients (r). For each comparison, ρ and r were determined with all datasets and after exclusion of outliers. Correlation coefficients between metrics were interpreted as follows: ρ or $|r| < 0.3$, no relationship; $0.3 \leq \rho$ or $|r| < 0.5$, weak relationship; $0.5 \leq \rho$ or $|r| < 0.7$, moderate relationship; $0.7 \leq \rho$ or $|r|$, strong relationship (21). The median and interquartile range for each metric were also determined.

Last, datasets included all NPs and three NP subsets defined as liposomes and solid lipid NPs (liposome subset); polymeric NPs—including micelles, hydrogels, and dendrimers—(polymeric subset); and inorganic, graphene, hybrid, or other NPs (inorganic subset). Statistical analysis as above was repeated for each NP type subset.

SUPPLEMENTARY MATERIALS

Supplementary material for this article is available at <http://advances.sciencemag.org/cgi/content/full/6/29/eaay9249/DC1>

[View/request a protocol for this paper from Bio-protocol.](#)

REFERENCES AND NOTES

1. S. E. McNeil, Unique benefits of nanotechnology to drug delivery and diagnostics. *Methods Mol. Biol.* **697**, 3–8 (2011).
2. S. E. McNeil, Challenges for nanoparticle characterization. *Methods Mol. Biol.* **697**, 9–15 (2011).
3. L. Yan, F. Zhao, J. Wang, Y. Zu, Z. Gu, Y. Zhao, A safe-by-design strategy towards safer nanomaterials in nanomedicines. *Adv. Mater.* **31**, e1805391 (2019).
4. U. Prabhakar, H. Maeda, R. K. Jain, E. M. Sevick-Muraca, W. Zamboni, O. C. Farokhzad, S. T. Barry, A. Gabizon, P. Grodzinski, D. C. Blakey, Challenges and key considerations

- of the enhanced permeability and retention effect for nanomedicine drug delivery in oncology. *Cancer Res.* **73**, 2412–2417 (2013).
5. W. C. Zamboni, V. Torchilin, A. K. Patri, J. Hrkach, S. Stern, R. Lee, A. Nel, N. J. Panaro, P. Grodzinski, Best practices in cancer nanotechnology: Perspective from NCI nanotechnology alliance. *Clin. Cancer Res.* **18**, 3229–3241 (2012).
 6. G. Song, D. B. Darr, C. M. Santos, M. Ross, A. Valdivia, J. L. Jordan, B. R. Midkiff, S. Cohen, N. Nikolaishvili-Feinberg, C. R. Miller, T. K. Tarrant, A. B. Rogers, A. C. Dudley, C. M. Perou, W. C. Zamboni, Effects of tumor microenvironment heterogeneity on nanoparticle disposition and efficacy in breast cancer tumor models. *Clin. Cancer Res.* **20**, 6083–6095 (2014).
 7. V. V. Ambardekar, S. T. Stern, NBCD pharmacokinetics and bioanalytical methods to measure drug release, in *Non-Biological Complex Drugs; the Science and the Regulatory Landscape* (Springer International Publishing, ed. 1, 2015), pp. 261–287.
 8. W. C. Zamboni, S. Strychor, E. Joseph, D. R. Walsh, B. A. Zamboni, R. A. Parise, M. E. Tonda, N. Y. Yu, C. Engbers, J. L. Eiseman, Plasma, tumor, and tissue disposition of STEALTH liposomal CKD-602 (S-CKD602) and nonliposomal CKD-602 in mice bearing A375 human melanoma xenografts. *Clin. Cancer Res.* **13**, 7217–7223 (2007).
 9. W. C. Zamboni, Concept and clinical evaluation of carrier-mediated anticancer agents. *Oncologist* **13**, 248–260 (2008).
 10. S. Ait-Oudhia, D. E. Mager, R. M. Straubinger, Application of pharmacokinetic and pharmacodynamic analysis to the development of liposomal formulations for oncology. *Pharmaceutics* **6**, 137–174 (2014).
 11. S. L. Skoczen, K. S. Snapp, R. M. Crist, D. Kozak, X. Jiang, H. Liu, S. T. Stern, Distinguishing pharmacokinetics of marketed nanomedicine formulations using a stable isotope tracer assay. *ACS Pharmacol. Transl. Sci.*, 10.1021/acspstsci.0c00011, (2020).
 12. H. He, D. Yuan, Y. Wu, Y. Cao, Pharmacokinetics and pharmacodynamics modeling and simulation systems to support the development and regulation of liposomal drugs. *Pharmaceutics* **11**, 110 (2019).
 13. A. T. Lucas, A. J. Madden, W. C. Zamboni, Formulation and physiologic factors affecting the pharmacology of carrier-mediated anticancer agents. *Expert Opin. Drug Metab. Toxicol.* **11**, 1419–1433 (2015).
 14. R. K. Jain, T. Stylianopoulos, Delivering nanomedicine to solid tumors. *Nat. Rev. Clin. Oncol.* **7**, 653–664 (2010).
 15. R. K. Jain, Normalizing tumor microenvironment to treat cancer: Bench to bedside to biomarkers. *J. Clin. Oncol.* **31**, 2205–2218 (2013).
 16. J. Liu, S. Liao, B. Diop-Frimpong, W. Chen, S. Goel, K. Naxerova, M. Ancukiewicz, Y. Boucher, R. K. Jain, L. Xu, TGF- β blockade improves the distribution and efficacy of therapeutics in breast carcinoma by normalizing the tumor stroma. *Proc. Natl. Acad. Sci. U.S.A.* **109**, 16618–16623 (2012).
 17. H. Maeda, H. Nakamura, J. Fang, The EPR effect for macromolecular drug delivery to solid tumors: Improvement of tumor uptake, lowering of systemic toxicity, and distinct tumor imaging in vivo. *Adv. Drug Deliv. Rev.* **65**, 71–79 (2013).
 18. A. J. Madden, S. Rawal, K. Sandison, R. Schell, A. Schorzman, A. Deal, L. Feng, P. Ma, R. Mumper, J. DeSimone, W. C. Zamboni, Evaluation of the efficiency of tumor and tissue delivery of carrier-mediated agents (CMA) and small molecule (SM) agents in mice using a novel pharmacokinetic (PK) metric: Relative distribution index over time (RDI-OT). *J. Nanopart. Res.* **16**, 2662 (2014).
 19. S. Wilhelm, A. J. Tavares, Q. Dai, S. Ohta, J. Audet, H. F. Dvorak, W. C. W. Chan, Analysis of nanoparticle delivery to tumours. *Nat. Rev. Mater.* **1**, 16014 (2016).
 20. S. E. McNeil, Evaluation of nanomedicines: Stick to the basics. *Nat. Rev. Mater.* **1**, 16073 (2016).
 21. M. M. Mukaka, Statistics corner: A guide to appropriate use of correlation coefficient in medical research. *Malawi Med. J.* **24**, 69–71 (2012).

Acknowledgments

Funding: This study was supported by NIH Carolina Center of Cancer Nanotechnology Excellence 1U54CA19899-01 Pilot Grant and T32 Carolina Cancer Nanotechnology Training Program 1T32CA196589 and R01CA184088. **Author contributions:** L.S.L.P., S.T.S., A.V.K., and W.C.Z. designed the study. L.S.L.P. collected the data. L.S.L.P. and A.M.D. performed the statistical analysis. L.S.L.P. and W.C.Z. drafted the manuscript. All authors contributed to the interpretation of the results and to the final manuscript text. This manuscript reflects the views of the authors and should not be construed to represent the US Food and Drug Administration's views or policies. **Competing interests:** The authors declare that they have no competing interests. **Data and materials availability:** All data needed to evaluate the conclusions in the paper are present in the paper and/or the Supplementary Materials. Additional data related to this paper may be requested from the authors.

Submitted 30 July 2019

Accepted 29 May 2020

Published 15 July 2020

10.1126/sciadv.aay9249

Citation: L. S. L. Price, S. T. Stern, A. M. Deal, A. V. Kabanov, W. C. Zamboni, A reanalysis of nanoparticle tumor delivery using classical pharmacokinetic metrics. *Sci. Adv.* **6**, eaay9249 (2020).

A reanalysis of nanoparticle tumor delivery using classical pharmacokinetic metrics

Lauren S. L. Price, Stephan T. Stern, Allison M. Deal, Alexander V. Kabanov and William C. Zamboni

Sci Adv **6** (29), eaay9249.

DOI: 10.1126/sciadv.aay9249

ARTICLE TOOLS

<http://advances.sciencemag.org/content/6/29/eaay9249>

SUPPLEMENTARY MATERIALS

<http://advances.sciencemag.org/content/suppl/2020/07/13/6.29.eaay9249.DC1>

REFERENCES

This article cites 19 articles, 7 of which you can access for free
<http://advances.sciencemag.org/content/6/29/eaay9249#BIBL>

PERMISSIONS

<http://www.sciencemag.org/help/reprints-and-permissions>

Use of this article is subject to the [Terms of Service](#)

Science Advances (ISSN 2375-2548) is published by the American Association for the Advancement of Science, 1200 New York Avenue NW, Washington, DC 20005. The title *Science Advances* is a registered trademark of AAAS.

Copyright © 2020 The Authors, some rights reserved; exclusive licensee American Association for the Advancement of Science. No claim to original U.S. Government Works. Distributed under a Creative Commons Attribution NonCommercial License 4.0 (CC BY-NC).